SUPLEMENT :
APPENDIX E

UTILIZATION OF THE THERMOMECHANICAL EFFECT AND OF THE MECHANO - CALORIC EFFECT FOR He II - COOLED MAGNETS *

Abstract

Superconducting magnets may exhibit a significantly extended critical surface when the operating temperature is lowered e.g. with NbTi-based alloys. Further, stability associated with superconductor-coolant interaction is enhanced in superfluid Helium-4 (= He II), provided the coolant ducts have been optimized. He II use has been promoted in several large systems. The present work investigates the magnet cryosystem options which utilize the thermomechanical effect of He II (fountain effect) and the mechano-caloric effect.

---

*) This "Supplement" is co-authored by W.E.W. Chen and T.H.K. Frederking Univ. Calif. Los Angeles and S. Caspi, Lawrence Berkeley Lab., Berkeley CA 94720. It is an extended version of a contribution to the 10th Intern. Magnet Technology Conf. MT-10 , Boston Sept. 1987, paper BQ-4.

1. Introduction

The thermodynamic effect discovered by Allen and Jones [1] is a unique property of superfluids. The He II thermomechanics is characterized by the external application of a temperature difference (ΔT) which creates a pressure difference (ΔP). The London equation predicts

$$\Delta P = \int dP = \int \rho S \, dT \tag{1}$$

(ρ liquid density, S entropy per unit mass). The temperature has to be below 2.17 K, the lambda temperature of saturated liquid Helium-4. The inverse of the effect is called the mechano-caloric effect. The process takes place in both cases at constant chemical potential (μ). For suitable arrangements, the temperature is lowered according to the equation

$$(\partial T/\partial P)\mu = \rho S \tag{2}$$

About 50 years have passed since the discovery, and utilization of the effects has been confined mostly to low-T laboratories. However, in recent years space technology and magnet technology development work has been initiated with the goal of utilizing the special advantages of the He II thermomechanics. The progress has come along in particular with NbTi magnets designed to bring fields to about 10 tesla with NbTi sections. Space cryogenics efforts have aided considerably in the understanding of several devices developed in the area, e.g. vapor-liquid phase separators.

2. Magnet Stability Enhancement in He II

The special properties of the coolant He II have permitted unusual stability margins for bath cooling of magnets. The coolant is characterized by a powerful internal mechanism ascribed to two-fluid flow properties which permit counterconvection. This creates rapid entropy removal in wide coolant ducts. The two-fluid system has superfluid moving toward "hot" spots and normal fluid convecting entropy away from these locations. The bath cooling preferred up to this time implies "zero net mass flow" (ZNMF) of the two-fluid system. ZNMF is similar to a heat pipe as there is a large rate of thermal energy transported per time, length and temperature difference. The coolant duct diameters have to be in range in order to take advantage of this special He II mechanism.

The stability improvement, potentially possible, is illustrated in Figure 1 which presents the response to a step input in power of small samples (e.g. winding sections [1]). The heat flux density q (per unit area of wetted surface) is shown as a function of "take-off time" (t_t). The latter marks the instant in a temperature (T) - time (t) thermogram at which the sample undergoes a T-excursion toward a quench of the superconducting state. The He II data are from Ref. 2. The He I data have been compiled elsewhere [3]. It is seen that there is an order of magnitude improvement in the take-off conditions despite a rather small change in the liquid density of the coolant. The inset of Fig. 1 shows q(t) and T(t) schematically.

Bath cooling improvements relying on He II have been achieved primarily with NbTi-based magnets. Related He II processing systems have been developed e.g. [4,5]. Despite the excellent internal convection mechanism, stability concerns have arisen for the occurrence of He I and vapor. Non-superfluid domains may have to be removed in some stability scenarios, and it takes some time to remove these "high-T" fluid domains. Therefore forced convection has come into focus. The forced flow mode may be generated in He II by thermomechanical pump action. The ΔT needed may be taken from heat leaks and dissipation of the magnet system itself. System options taking advantage of this He II property have been proposed recently [6]. It is the purpose of the present studies to

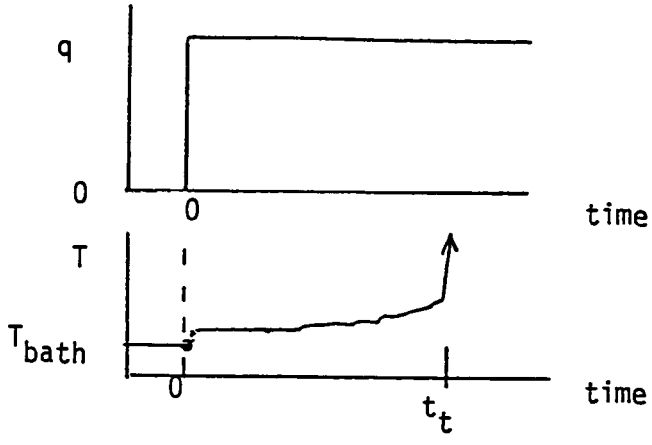

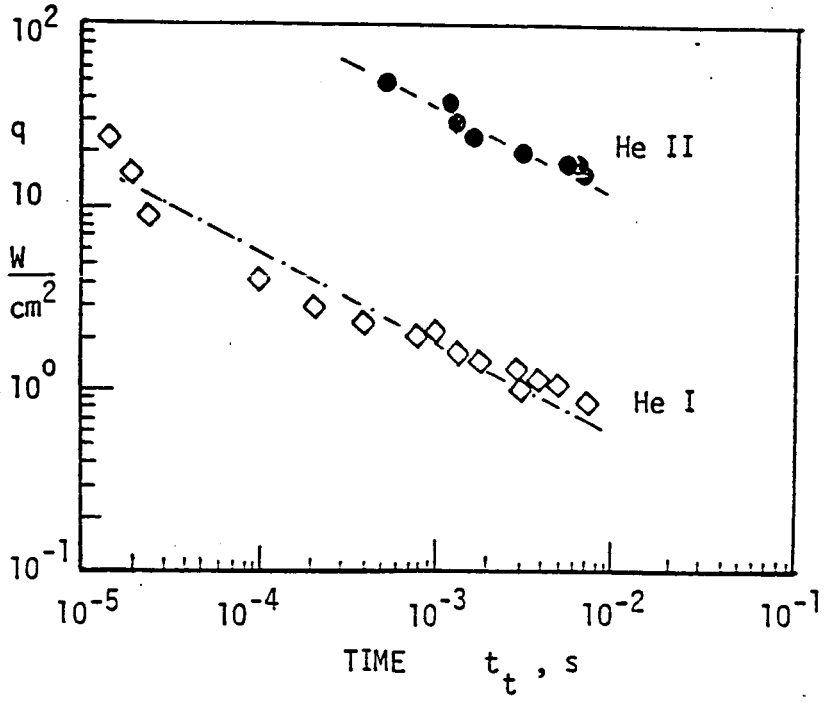

Fig. 1. Thermogram results for step input in power (heat flux density q): q as a function of time (t) at "take-off " conditions; He II , Ref.[1]; He I data compilation [2].

Inset : a. q- step ; b. Temperature versus time with initial low ΔT region (schematically) and take-off at t_t .

investigate cryosystem options relying on the use of the thermomechanical effect, and its inverse for refrigeration [7] (called vortex refrigeration). In addition, the possibility of heat leak interception by thermomechanical means is included.

3. He II Production and Cyclic Operation

Various steps are considered including an outline of present magnet coolant processing approaches.

Existing Systems: The development of He II refrigeration systems (e.g. [4,5]) has relied on Joule-Thomson (JT) throttling using the latent heat of vaporization. Vacuum pump power is needed for the operation. In contrast, the vortex refrigeration does not need such a large amount of mechanical power when operational. It is noted that both JT and VR systems do not have moving parts in the He II production facility.

Thermodynamic Cycle: The vortex refrigerator has been introduced by Staas and Severijns [7] aiming at the attainment of low temperatures. Concerning refrigeration near 2 K , there are quite a few cycle options available. For the present purpose we adopt an ideal sequence of states noting that no performance numbers, such as COP have been given so far [7]. The cycle is characterized by the four changes μ–P–μ–P. There are two isobars P = const, and two isopotential state changes at constant chemical potential μ. The cycle is shown schematically in the temperature-entropy (S) diagram (Fig. 2). Table I presents other details. The change at $d\mu = 0$ is a peculiarity of He II. If shedding of

Table I. Ideal thermodynamic cycle : μ - P - μ - P

STATE CHANGE $i \rightarrow j$	THERMODYNAMIC PATH	SUBSYSTEM
$1 \rightarrow 2$	CONSTANT CHEMICAL POTENTIAL	THERMOMECHANICAL POROUS PLUG
$2 \rightarrow 3$	ISOBAR	HEAT EXCHANGER (AFTERCOOLER)
$3 \rightarrow 4$	CONSTANT CHEMICAL POTENTIAL	MECHANO-CALORIC POROUS PLUG
$4 \rightarrow 5$	ISOBAR	HEAT EXCHANGER (REFRIGERATION)

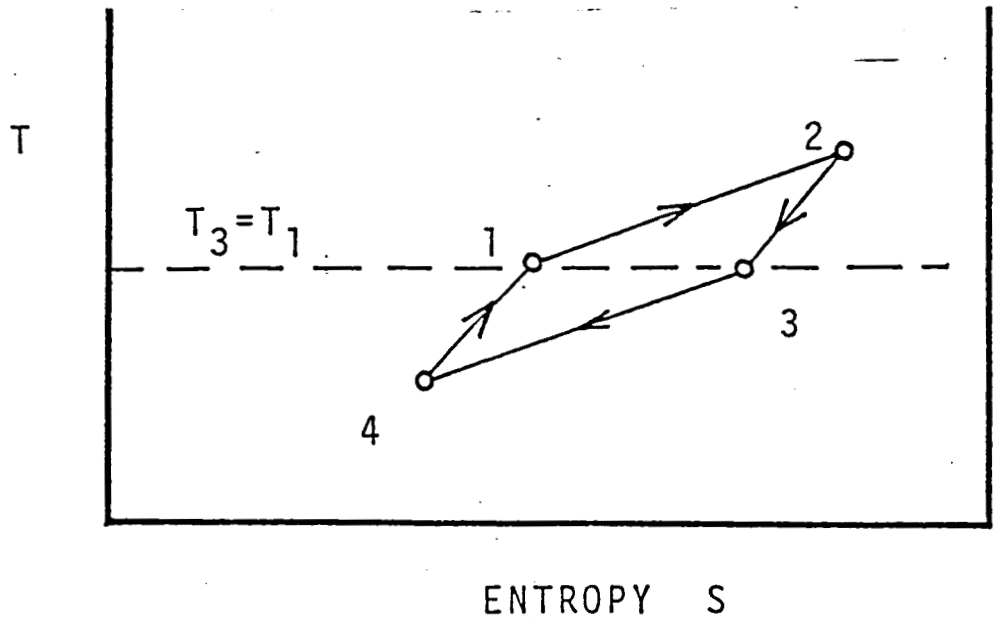

Fig. 2. Ideal thermodynamic cycle for vortex refrigerator in the temperature-entropy diagram (schematically in logarithmic coordinates).

quantum vortices takes place, such that they cross the stream lines of fluid flow, there will be a change in chemical potential (Anderson's theorem). Thus, the absence of such a change implies that there is no vortex shedding. The device producing this ideal condition has been called "ideal superleak" (ISL). The pressure is raised from point 1 to point 2 by the thermomechanical effect described by London's equation (1). In the change from point 3 to point 4 the lowering of the pressure is associated with $dT < 0$ (mechano-caloric effect).

The set of changes $1 \rightarrow 2$ and $3 \rightarrow 4$ constitutes a subsystem called "power unit" (Fig. 3). It represents isothermal pressurization by heat supply. The other cycle portion ($3 \rightarrow 4$ and $4 \rightarrow 1$) is called "VR refrigeration subsystem".

Power Unit: The simple cycle adopted contains the special condition $T_3 = T_1$. Therefore the power unit is a fountain effect pump (FEP) with an aftercooler downstream (change $2 \rightarrow 3$). Pressurization is achieved by the heat supply of T_2S_2 for the ISL-case. An isobaric ideal heat exchanger is adopted for the subsequent cooling process. The ideal energetics of the ISL-facilitated FEP is displayed in Fig. 4 in normalized form [8]. The quantity $\bar{\varepsilon}_e$ is the (normalized) ratio of the flow power achieved to the heat input for constant mass flow (zero mass loss). Figure 4 shows that $\bar{\varepsilon}_e$ tends toward an asymptotic value as ΔT is raised. The absolute maximum of this energetic effectiveness is about 15%. Experiments conducted in recent time [9] indicate small departures from the ideal performance. In other words, the efficiency with respect to ISL may be high, e.g. 80% when fine porous media are used as pump plugs.

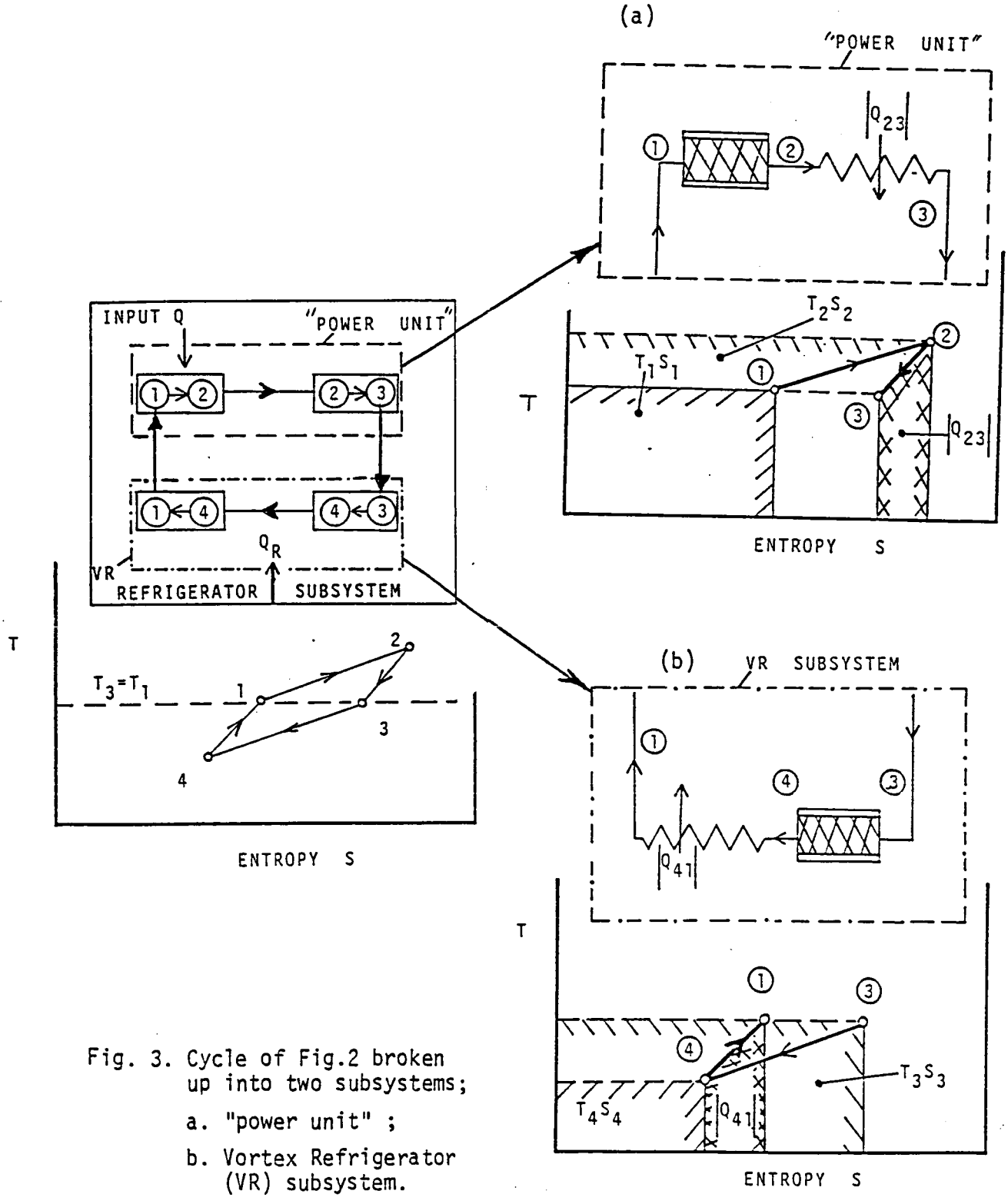

Fig. 3. Cycle of Fig.2 broken up into two subsystems;

a. "power unit" ;

b. Vortex Refrigerator (VR) subsystem.

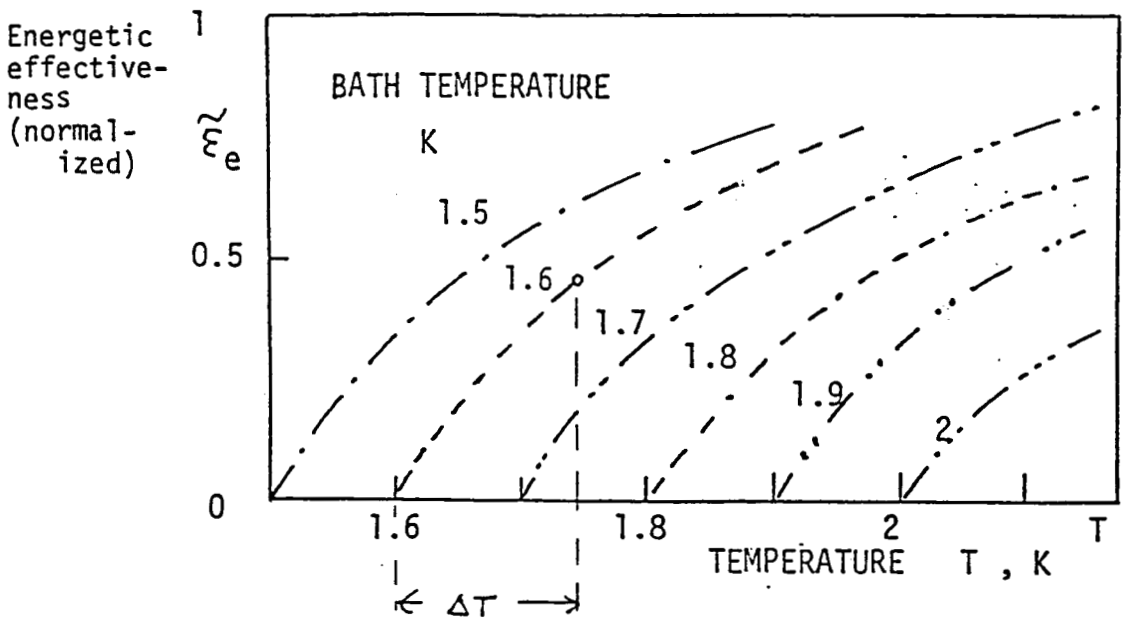

Fig. 4 . Energetic effectiveness, normalized in terms of the ultimate asymptotic value of about 15 % .
The point o on the 1.6 K bath isotherm ($T = T_1$) indicates the temperature difference and the $\tilde{\varepsilon}_e$ - value at that ΔT.
Details have been given in Ref. [8].

VR Refrigerator Subsystem. The temperature T_4 of the μ–P–μ–P cycle is the lowest temperature achievable ideally. This temperature is shown in Fig. 5 as a function of the initial temperature T_1. It is seen that a significant lowering of T is available at low T_1. The refrigeration load T_4S_4 is achieved ideally. Subsequently the change from point 4 to point 1 again is adopted as ideal isobaric change. For the purpose of cycle quantification, both the contribution T_4S_4 and the heat supply Q_{41}, for the change $4 \rightarrow 1$, are considered useful for the determination of the coefficient of performance (COP_{VR}). With this assumption we have a total refrigeration load, ideally available, of

$$Q_R = T_4S_4 + Q_{41} \tag{3}$$

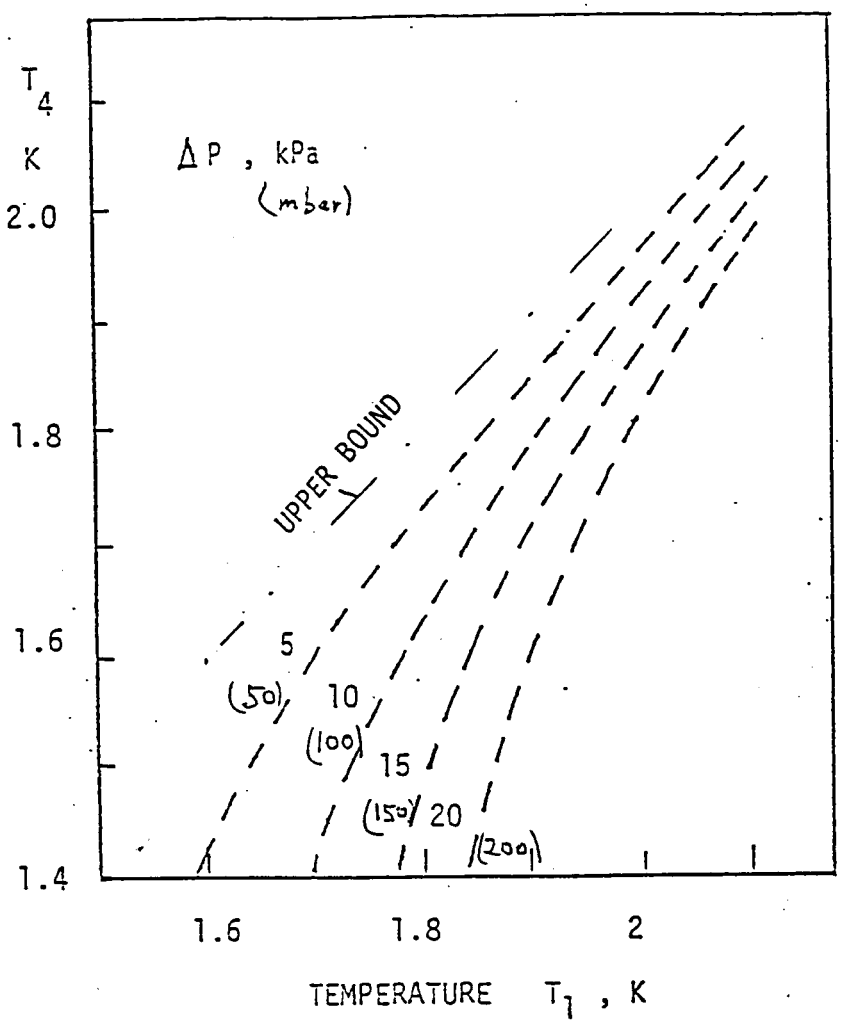

Fig. 5. Ideal cold end temperature T_4 achieved in the μ–P–μ–P VR cycle, versus initial temperature T_1 ("bath temperature"), for various pressure increases i the fountain effect pump (ideal FEP)

Coefficient of Performance: The definition adopted is consistent with similar heat utilization schemes at elevated temperatures aiming at heat pumping.* Thus, we introduce the COP_{VR} as the ratio of the refrigeration energy to the heat input:

$$COP_{VR} = [T_4S_4+Q_{41}]/T_2S_2 \qquad (4)$$

The results are shown in Fig. 6 for various pressure increases achieved in the power unit. The COP is seen to be a monotonically increasing function of T_1 for a specified ΔP.

*) Examples are waste heat utilization with absorption refrigeration systems and solar - powered refrigeration systems using photon radiation (instead of photo-voltaics).

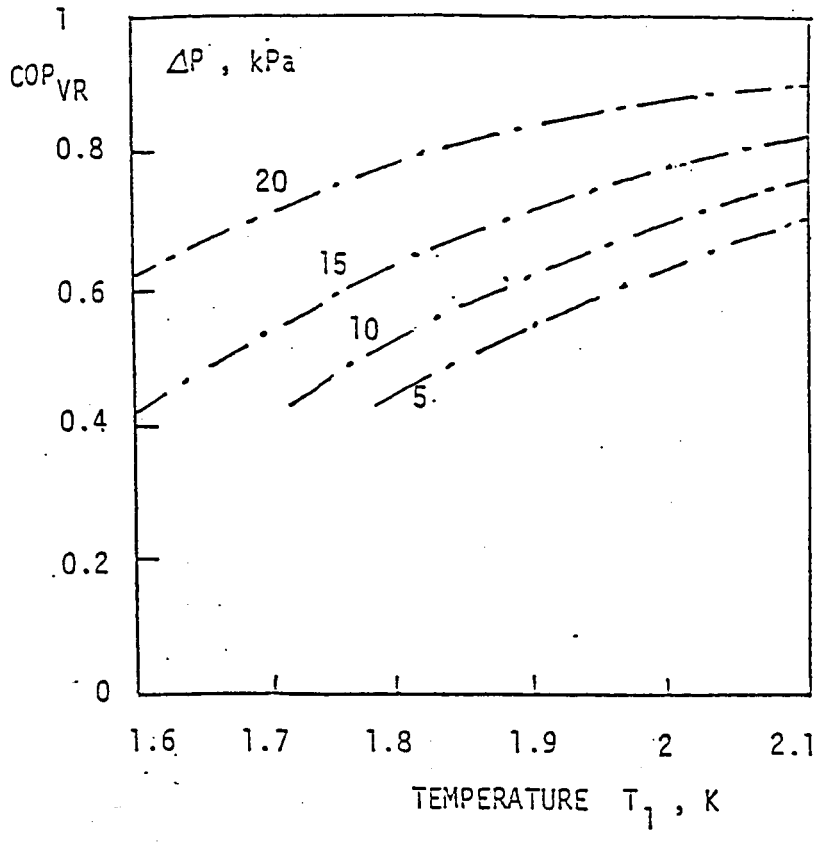

Fig. 6. Coefficient of performance, COP_{VR}, of the ideal vortex refrigerator as a function of T_2 for various pressure increases.

He I-He II Production. The VR system operates in He II. Therefore, in principle a He I stage is needed. Hofmann et al. [9] have shown that a local He I domain may be tolerated as long as major portions of the magnet cooling system are below 2.17 K. Thus a certain insensitivity to local T-excursions is indicated.

The Claudet et al. system [4] needs large amounts of power when the refrigeration load is raised from the order of 100 Watts to 1 kW. This constraint and other concerns have led to cold vapor compression in the "Tore Supra" system. In the He I range, obviously a "classical" system is needed prior to the startup of a vortex refrigerator. The advantage of VR is the replacement of the He II range-related mechanical power by heat input, suitably taken from room temperature enclosures of the magnet system, or from lower temperatures. Therefore, power savings appear to be attractive as soon as a suitable VR system has been introduced as replacement.

Concerning ideal cycle implementation, it is noted that multi-stage operation and heat exchanger use will be beneficial.* A 4-stage pump has been operated by Severijns for a dilution refrigerator [10]. Thus, the process is brought closer to Carnot cycle performance.

*Examples in this area have been discussed at the 1986 Cryocooler Conference, and a two-stage pump for space conditions has been proposed by Kittel.

In the He I range, the JT throttling has been supplemented recently by vapor-liquid phase separation in passive (porous plug), e.g. [11], and active (slit geometry) devices. Therefore, several tools are available for the subsystem selection replacing the traditional He II production schemes for magnet cooling purposes.

4. Heat Leak Interception

The use of the He II thermomechanics derived from heat leaks has been proposed by Hofmann [6] aiming in particular at forced flow. A pressurized system has been selected and experimentally documented for this purpose [9]. An additional option is heat leak interception at current leads, supports and other devices. In the present section, several features are outlined for this type of heat leak interception.

The principle of operation is quite similar to cooling by vapor generated from a He I bath near 1 atm. Instead of vapor, liquid is used to be directed in counterflow to the heat flow direction. Again the thermomechanics utilized is restricted to the He II range noting the exceptions found in the Hofmann et al. experiments [9]. The ideal change of state is characterized by $d\mu = 0$. This constraint may be expressed as equality for the enthalpy difference and the temperature-entropy terms:

$$\Delta H = \Delta(T\,S) \tag{5}$$

Calculation for vapor-cooled supports have included the ideal case of zero thermal resistance at the solid-vapor boundary. Simple solutions obtained for this limit provide the best heat leak reduction. A similarly simple bound on the heat leak reduction in He II results from the zero thermal resistance solution.

Figures 7 and 8 show the two cases of vapor cooling and He II cooling schematically. In the latter case a suitable porous medium is employed. A fraction of the He II mass is taken out of the cold bath. It moves along the support or current lead in a porous layer. Subsequently, the liquid may enter a "lambda shield" exiting via phase separator into vapor cooled shields. Another option is the conversion into He I and continued coolant flow along the support/current lead to a higher T-level.

The ISL model case requires a thermal energy rejection rate at the cold end location involving (T S) at that temperature. Obviously, if heat leak interception would be the only factor to be considered, the lowest T possible requires the smallest heat rejection rate.

On the warm side of the He II heat leak interception, latent heat utilization appears to be another possibility. The best location for this first order phase conversion is expected to depend on details of the transport processes involved in the porous media fluid dynamics.

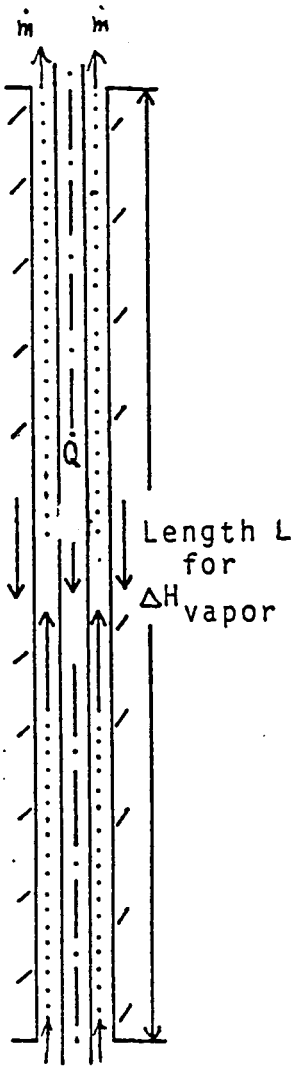

Fig. 7. Schematic setup for "classical"vapor cooling of current leads with counterflow of heat ($\dot{Q}$) and vapor mass flow ($\dot{m}$). Ideally the length L produces a T-increase associated with the entire enthalpy difference available with the vapor flow.

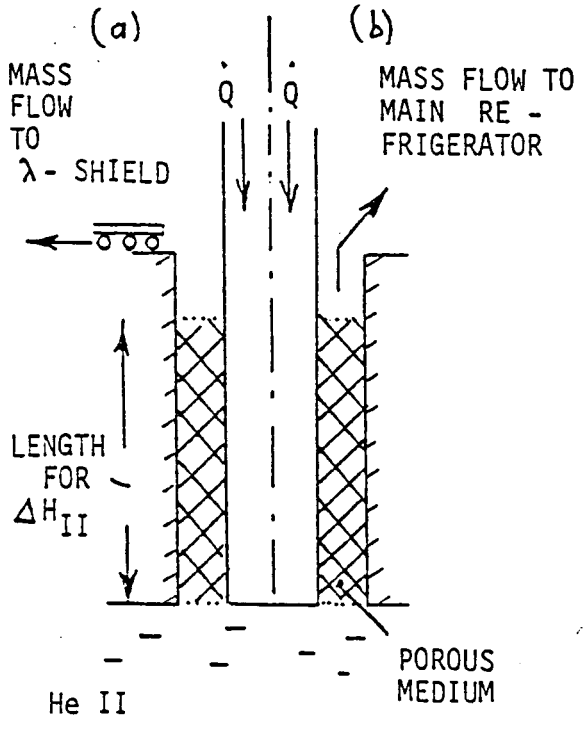

Fig. 8. Schematic diagram for He II cooled rods or current lead sections. ΔH_{II} is the enthalpy difference available in the He II region

5. Experiments

Heat transfer limitations appear to be among the important constraints for the thermomechanics of He II-cooled magnets. Therefore, our experimental work has addressed two items in this area, the mass flow rate as a function of ΔT in the real FEP [12], and the T-distribution in a specifically chosen heat transfer unit [13]. The latter has packed copper powder. An example of the T-distributions obtained is shown in Fig. 9. The heat transfer unit is depicted in the inset of Fig. 9. The FEP upstream has a fine pressured aluminum oxide plug. The temperature T_1 is measured upstream, the temperature T_2 is the downstream value, and T_o is the temperature in the center of the unit. The flow rate, given as superficial velocity of the FEP, has been at the order of 2 to 10 cm/s. The absolute flow rate is listed in the inset of Fig. 9.

In nearly all of the runs a monotonic decrease of the temperature toward the downstream end of the heat transfer unit has been observed. Thus, leakage of thermal energy is indicated by the records. This behavior is influenced noticeably by the pore size of the porous medium [11]. The related continuum equations for non-linear flow suggest a remedy for heat leak prevention. It has been

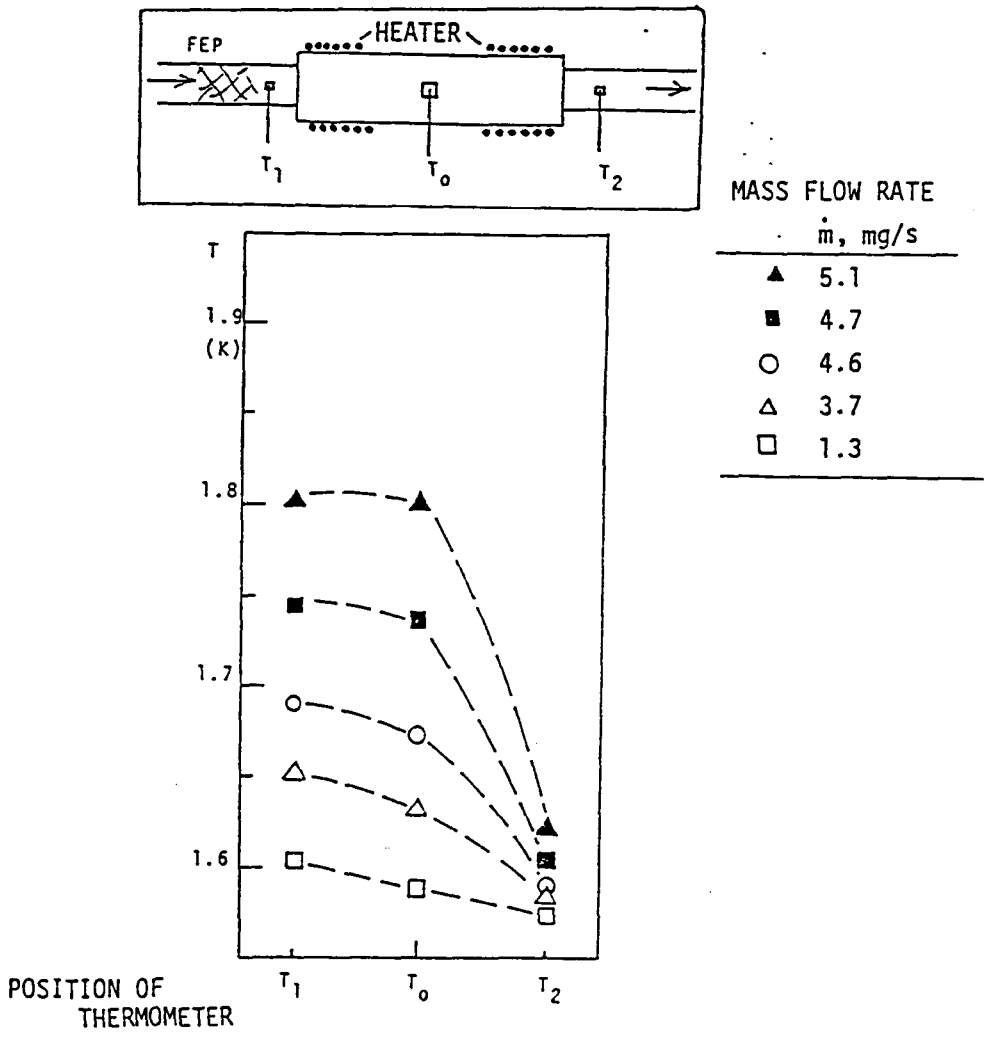

Fig.9. T-distributions in the FEP unit ; inset : heater geometry, schematic.; heater section Fig.10 shows the apparatus.

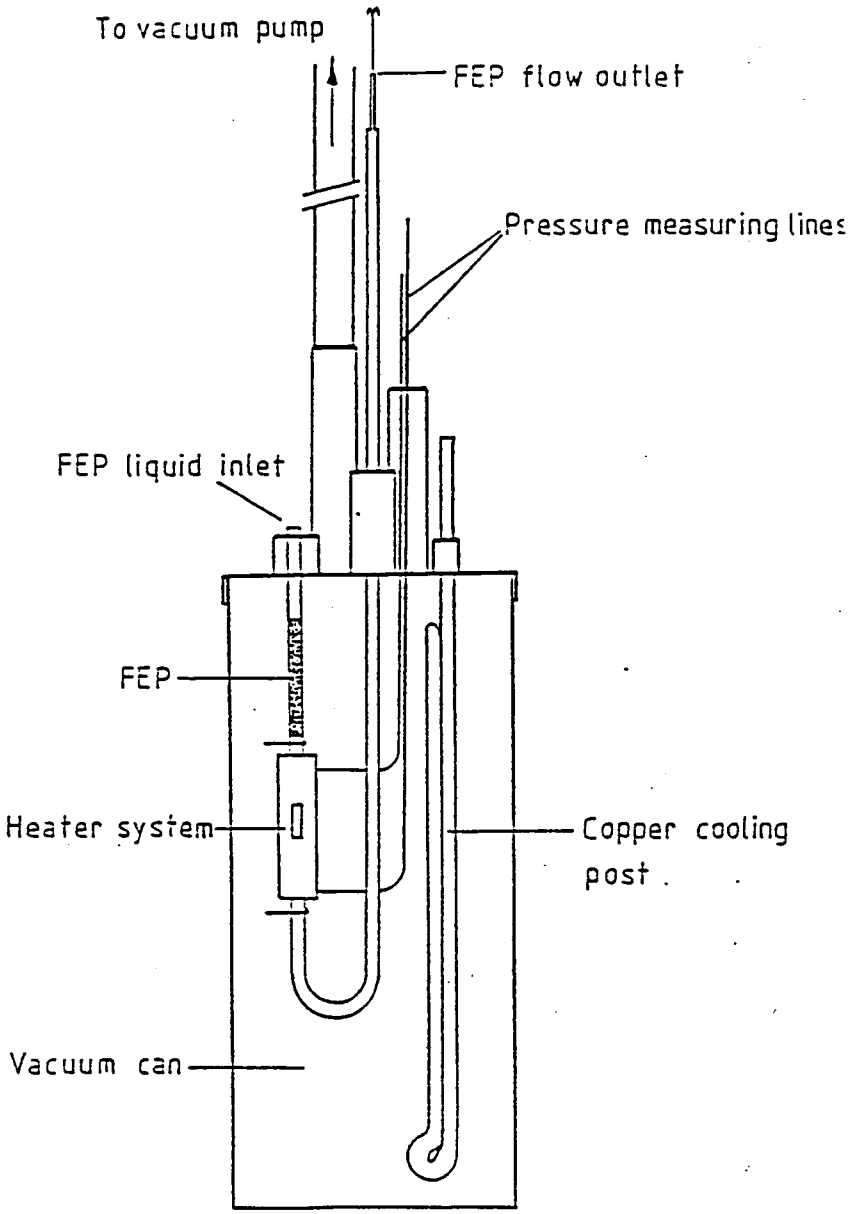

Fig. 10. Apparatus , schematically . Further details are in Ref.13.

proposed [13] to install a special end plug at the downstream side. This plug with very fine pores and suitable dimensions has the purpose of preventing low efficiencies of heat input utilization for improved magnet cryogenics.

The handling of heat input, converted to flow power in the "power unit", and subsequent depressurization in the mechano-caloric device involves considerable heat transfer problems. The term (T S) is reasonably large at temperatures not too far from the lambda temperature. Further, the critical current density of NbTi is rather flat as T is changed to low T. Therefore, the operation not too far from the lambda point appears to bring about good ideal COP values. The real system behavior will depend on the suppression of irreversibilities, and optimum heat transfer appears to be very desirable to keep the real system performance high. Therefore, additional knowledge of the thermal aspects is considered very useful.

6. Discussion

The various thermomechanics options in magnets may be subdivided into three classes: forced flow in magnet windings, heat leak interception, and vortex refrigeration (with its different variations). The first two items appear to require only the "power unit" while the third one needs a mechano-caloric subsystem. In any case all of the magnet related options need heat transfer and thermodynamic knowledge of the process details.

At this point the question may come up why traditional cryocooler literature apparently has omitted the Staas-Severijns vortex cooler. Another question is related to the lack of COP information until very recently. It is believed that part of this lack of knowledge resides in some simplifications of the two-fluid model which let "zero Kelvin superfluid" flow through the ISL device, and apparent lack of local equilibrium.

The real porous plug (called also "superfilter" in some papers) has been probed with thermometers. The T-results obtained always show *local equilibrium, i.e. the normal fluid excitations are* generated at a sufficiently high rate for the establishment of equilibrium. Thus the thermometer shows a continuous temperature profile response in line with the cycle calculations presented above. To overcome some of the literal, purely hydrodynamic interpretations of the two fluid model, one may visualize the processes as the result of excitation generation constrained by a "pseudo-reaction". Noting that the first order phase transition constitutes a limiting case of a chemical reaction, we recognize that inclusion of this "pseudo-reaction" picture enriches the classes of particle/charge transfer systems in thermodynamics and transport phenomena.

After establishment of the continuous T-profile it appears to be a minor step to introduce a differential element of the ISL*. The changeover to finite difference is just as useful when it comes to implementation of real pressurization and depressurization. Thus one may synthesize a system with n stages involving low conductivity porous ($d\mu = 0$) medium and a subsequent aftercooler medium (eg. sintered Cu and heat removal hookup). The final goal appears to be an integrated, taylored multi-stage unit with large surface area and small absolute size.

Going back to the hydrodynamics of the two-fluid model we recognize the superfluid speed as superficial porous media mean speed ($\vec{v}_{So}$). Locking of normal fluid ($v_{no} \rightarrow 0$) in the ISL implies a mass flux density of the flow of

$$|\vec{j}_o| = |\rho\vec{v}_o| = \rho_S\vec{v}_{So}| \tag{5}$$

where ρ_S is the superfluid density.

Thus, pseudo-reaction and hydrodynamics constraints aid in getting an understanding of the special design conditions involving the He II thermomechanics.

---

*In Ref. 8 such a differential element has been used to facilitate an understanding of approximations for the power unit treated as ISL.

7. Conclusions

The ideal coefficients of performances obtained are very encouraging. The COP comparison alone however is somewhat misleading as usually "efficiencies with respect to Carnot cycle" involve mechanical power. The present systems are attractive in so far as *no* mechanical power is involved in the He II portion of the system if the heat input naturally available all the way from 300 K down is utilized. Thus, the possibilities of magnet heat leak use for energetics and stability improvements are quite remarkable when He II is selected as magnet coolant.

Acknowledgments. The present studies have had the benefit of preceding space system investigations supported in part by NASA Ames Research Center. The present lab collaborators [14] have provided input. Further the following contributors are acknowledged: W. A. Hepler (FEP experiments), P. Khandhar (heat leak use), D. Y. Ono (cycle analysis).

References

[1] K. R. Atkins, Liquid Helium, Cambridge University Press, 1959.

[2] D. Gentile and W. V. Hassenzahl, Adv. Cryog. Eng., Vol. 25, pp. 385-392, 1980.

[3] Y. I. Kim et al., Appl. Phys. Letters, Vol. 43, pp. 451-453, 1983.

[4] G. Bon Mardion, G. Claudet, P. Seyfert and J. Verdier, Adv. Cryog. Eng., Vol. 23, pp. 358-362, 1978

[5] R. P. Warren, G. R. Lambertson, W. S. Gilbert, R. B. Meuser, S. Caspi and R. V. Schafer, Proc. 8th Int. Cryog. Eng. Conf. ICEC-8, IPC Sci. Technol., 1980, pp. 373-377.

[6] A. Hofmann, Proc. Int. Cryog. Eng. Conf. ICEC 11, Butterworths, pp. 306-311, 1986.

[7] F. A. Staas and A. P. Severijns, Cryogenics, Vol. 9, pp. 422-426, 1969.

[8] T. H. Frederking, P. Kittel, T. C. Nast, C. K. Liu, Proc. ICEC-11, pp. 323-330, 1986.

[9] A. Hofmann et al., Cryog. Eng. Conf. 1987, paper BC-5.

[10] A. P. Severijns, Cryogenics, Vol. 20, pp. 115-121, 1980.

[11] S. W. K. Yuan and T. H. K. Frederking, Cryogenics, Vol. 27, pp. 27-33, 1987.

[12] W. E. W. Chen, T. H. K. Frederking and W. A. Hepler, Cryog. Eng. Conf., St. Charles, IL, 1987, paper BC-6 (to be published, Adv. Cryog. Eng.).

[13] W. E. W. Chen, M.Sc. Thesis, Univ. Calif., Los Angeles, 1987.

[14] T. H. K. Frederking, P. Abbassi, F. Afifi et al., UCLA Rept. 8734, 1987.